OXFORD
SOT | Society of Toxicology
www.toxsci.oxfordjournals.org

TOXICOLOGICAL SCIENCES, 167(1), 2019, 105–115

doi: 10.1093/toxsci/kfy267
Advance Access Publication Date: October 29, 2018
Research Article

Heavy Metal Neurotoxicants Induce ALS-Linked TDP-43 Pathology

Peter E.A. Ash,[*,1] Uma Dhawan,[*,†,1] Samantha Boudeau,[*] Shuwen Lei,[*] Yari Carlomagno,[‡] Mark Knobel,[*] Louloua F.A. Al Mohanna,[*] Steven R. Boomhower,[§] M. Christopher Newland,[¶] David H. Sherr,[‖] and Benjamin Wolozin[*,|||,2]

[*]Department of Pharmacology and Experimental Therapeutics, Boston University School of Medicine, Boston, Massachusetts 02118; [†]Department of Biomedical Science, Bhaskaracharya College of Applied Sciences, University of Delhi, Delhi 110075, India; [‡]Neuroscience Division, Mayo Clinic, Jacksonville, Florida 32224; [§]Department of Environmental Health, Harvard T.H. Chan School of Public Health, Boston, Massachusetts 02115; [¶]Department of Psychology, Auburn University, Auburn, Alabama 36849; [‖]Department of Environmental Health, Boston University School of Public Health; and [|||]Department of Neurology, Boston University School of Medicine, Boston, Massachusetts 02118

[1]These authors contributed equally to this work.

[2]To whom correspondence should be addressed at Deparments of Pharmacology and Neurology, Boston University School of Medicine, 72 East Concord Street, R614, Boston, MA 02118-2526. Fax: 617 358 1599. E-mail: bwolozin@bu.edu.

ABSTRACT

Heavy metals, such as lead, mercury, and selenium, have been epidemiologically linked with a risk of ALS, but a molecular mechanism proving the connection has not been shown. A screen of putative developmental neurotoxins demonstrated that heavy metals (lead, mercury, and tin) trigger accumulation of TDP-43 into nuclear granules with concomitant loss of diffuse nuclear TDP-43. Lead (Pb) and methyl mercury (MeHg) disrupt the homeostasis of TDP-43 in neurons, resulting in increased levels of transcript and increased splicing activity of TDP-43. TDP-43 homeostasis is tightly regulated, and positively or negatively altering its splicing-suppressive activity has been shown to be deleterious to neurons. These changes are associated with the liquid-liquid phase separation of TDP-43 into nuclear bodies. We show that lead directly facilitates phase separation of TDP-43 in a dose-dependent manner in vitro, possibly explaining the means by which lead treatment results in neuronal nuclear granules. Metal toxicants also triggered the accumulation of insoluble TDP-43 in cultured cells and in the cortices of exposed mice. These results provide novel evidence of a direct mechanistic link between heavy metals, which are a commonly cited environmental risk of ALS, and molecular changes in TDP-43, the primary pathological protein accumulating in ALS.

Key words: TDP-43; neurotoxicity; metals; ALS; LLPS; neurodegeneration.

This article is published as part of the NTP Neurotoxicology Screening Strategies Initiative.

Amyotrophic lateral sclerosis (ALS) stems from the loss of descending motor neurons resulting in muscle degeneration and eventually death. In the large majority of ALS cases, motor neurons are observed to accumulate pathologic insoluble cytoplasmic and nuclear inclusions of TDP-43 (Arai *et al.*, 2006; Neumann *et al.*, 2006). TDP-43 inclusions also present as secondary pathology in varying degrees in a number of neurodegenerative diseases, including in frontotemporal dementia (Murray *et al.*, 2011), Alzheimer's disease (Uryu *et al.*, 2008), and Parkinson's disease (Nakashima-Yasuda *et al.*, 2007). TDP-43 is

© The Author(s) 2018. Published by Oxford University Press on behalf of the Society of Toxicology.
All rights reserved. For permissions, please e-mail: journals.permissions@oup.com

an RNA-binding protein (RBP) that exhibits both nuclear and cytoplasmic functions. It is predominantly localized to the nucleus under basal conditions, where it is involved in RNA splicing, as well as a multitude of other RNA metabolic functions (Ratti and Buratti, 2016). The presence of cytoplasmic and intranuclear inclusions may therefore produce neuronal toxicity through a gain of function or through disruption of physiological functions of TDP-43 in the nucleus, from which it is depleted. The causes of ALS are incompletely understood. While mutations in TDP-43 are associated with heritable ALS (Rutherford *et al.*, 2008; Sreedharan *et al.*, 2008), the 90%–95% of ALS cases that occur without a family history of the disease all demonstrate TDP-43 pathology post-mortem.

Environmental risk factors likely play an important role in ALS (Oskarsson *et al.*, 2015). Exposure to heavy metals (including lead, mercury, and selenium) (Beghi *et al.*, 2006; Trojsi *et al.*, 2013) increase odds ratios of developing ALS. Increased risk of ALS has been associated with increasing age, with gender, smoking, and diet (de Jong *et al.*, 2012; Morozova *et al.*, 2008; Wang *et al.*, 2011), with service in the military (Weisskopf *et al.*, 2005, 2015), and with exposure to toxins such as organophosphates in agricultural herbicides and pesticides (Das *et al.*, 2012). A ~100× fold increase in risk of a complex of disorders consisting Parkinsonism, dementia, and ALS has been connected to the consumption of the amino acid β-methylamino-L-alanine (BMAA) (Muñoz-Sáez *et al.*, 2015). Metals have also been associated with increased risk of other neurodegenerative disease such as Parkinson disease, Alzheimer's disease, and Wilson's disease (Bjorklund *et al.*, 2018; Squitti *et al.*, 2018). Airborne exposure to aromatic agonists of the aryl hydrocarbon receptor (AHR) have been linked to ALS (Ruder *et al.*, 2014; Malek *et al.*, 2015). We recently demonstrated that polycyclic aromatic hydrocarbons (PAHs) and other agonists of the AHR, including dioxins and planar polychlorinated biphenyls (PCBs), increases accumulation of TDP-43 in motor neuron differentiated iPSCs and in murine brain (Ash *et al.*, 2017). The link between AHR activators and TDP-43 accumulation raises the possibility that other environmental risk factors linked to ALS might contribute to TDP-43 pathology.

Due to time and resource constraints, it is challenging to test the large number of environmental compounds for their potential to cause neurodevelopmental and/or neurodegenerative changes using traditional in vivo methods. As such, the need to create a screening battery to prioritize compounds for further testing is well recognized (Aschner *et al.*, 2017; Bal-Price *et al.*, 2012; Crofton *et al.*, 2012; Fritsche *et al.*, 2018; Smirnova *et al.*, 2014). In this study, we assayed 91 putative neurodevelopmental toxins (National Toxicology Program high-throughput screen NeuroTox 91 Plate-Number: 4001204495) (Behl *et al.*, 2018) for their ability to trigger aggregation of TDP-43 in stably transfected rat PC12 cells. We observe that four toxicants, lead (II) acetate trihydrate, methyl mercuric (II) chloride, bis(tributyltin)oxide, and colchicine, produce a larger fraction of PC12 cells with TDP-43 aggregates. As lead and mercury have been linked epidemiologically with increased risk of ALS, we further investigated the consequences of exposure on the biochemistry and function of TDP-43. Lead and methyl mercury trigger formation of nuclear Tdp-43 inclusions in primary neurons. Exposure to lead and methyl mercury results in accumulation of insoluble Tdp-43 and dysregulation of its function in alternative splicing. Lead also promotes the liquid-liquid phase separation (LLPS) of TDP-43 in vitro. These important findings connect exposure to the heavy metals lead and mercury to the key pathological and molecular aberrations that occur in ALS, namely the aggregation of TDP-43 and its perturbed RNA metabolic functions. Furthermore, it demonstrates how a battery of screening platforms, including the PC12 cell line, might be used as a means to identify environmental neurotoxins that warrant further analysis in vivo.

MATERIALS AND METHODS

PC12 cell culture. Frozen stocks of rat PC12 cells that were stably transfected with Tet-off-inducible wild-type TDP-43::GFP (for details, see Boyd *et al.*, 2014) were thawed and grown in collagen-coated flasks (Thermo Fisher, 132708) in DMEM (4.5g/l glucose, L-glutamine, and sodium pyruvate; Corning 10-013-CV) with 10% horse serum (Gibco, 26050088), 5% Tet-free FBS (Atlanta Bio, S10350H), 10 μg/ml Pen/Strep (Gibco, 15140122), 0.1 mg/ml Hygromycin B (Gibco, 10687010), 0.1 mg/ml geneticin (Gibco, 10131027), and 1 μg/ml doxycycline for 72 h using standard cell culture techniques. TDP-43:: GFP expression was induced by aspirating the flask and replacing with induction media lacking doxycycline for 72 h. For each screening experiment, the induced PC12 cells were plated into 5 collagen-coated 96-well plates (Corning, 354407) (3×10^4 cells/well) in 100 μl induction media. No cells were plated in wells on the first and the last row of plates. As negative controls, uninduced cells were plated in wells B2, B3, C2, and C3 of plate 1 in each experiment. After overnight incubation, the cells were treated with compounds.

NTP HTS NeuroTox compound screening. The assay screened 91 compounds received from NIEHS (NTP HTS NeuroTox 91 Plate-Number: 4001204495) (Behl *et al.*, 2018) in TDP-43:: GFP expressing PC12 cells. The compounds were suspended at ~20 μM in DMSO (except compounds C7 and C10) and were provided in 0.75 ml alphanumeric screwcap tubes in 96-vial plate rack thereby blinding the researcher to the compound. Induced PC12 cells were treated for 18–20 h with compounds in four doses: 100, 25, 6.25, and 1.56 μM in quadruplicate. Cells treated with compounds C7 and C10 received 6.25, 1.56, 0.39, and 0.1 μM treatments in quadruplicate. In each experiment consisting of five 96-well plates, 18 compounds were assayed. In each plate, triplicate wells were treated with 0.125% DMSO (vehicle) and 15 μM sodium arsenite (with 0.125% DMSO) as negative and positive controls of TDP-43:: GFP aggregation and to permit normalization across plates.

PC12 image acquisition and statistical analysis. Following treatment, the plates were washed twice with phosphate-buffered saline (PBS) before fixing with 4% PFA in PBS for 20 min at 4°C. The fixed cells were washed with cold PBS, counterstained with 0.5 μg/ml DAPI in PBS and stored at 4°C until imaging (less than 48 h). The 96-well plates were imaged on an IN Cell Analyzer 2000 (GE Healthcare) by 50 ms acquisition in the DAPI and GFP channels from 9 preselected random fields in each well. Images were analyzed using IN Cell Workstation software (GE Healthcare). Cells were segmented using an algorithm wherein DAPI-stained nuclei were defined with a minimal area of 22 μm^2 and a periphery of 5 μm. Cell viability under compound treatment was quantified by nuclei count. Details of image segmentation analysis of TDP-43:: GFP diffuse and punctate phenotypes was previously described in Boyd *et al.* (2014). The proportion of cells with diffuse and/or punctate TDP-43:: GFP was quantified giving 4 feature outputs: (1) cell viability; (2) % diffuse cells with diffuse TDP-43:: GFP; (3) % punctate TDP-43:: GFP/cell; and

(4) ratio of "% diffuse TDP-43:: GFP":"% punctate TDP-43:: GFP". Mean ± 2*SD* cell count of the 9 imaging fields per well were calculated and outliers excluded. Outliers were observed in 20%–50% of the wells across the experiments; in particular, field no. 3 (located in the well where aspiration occurred) was a frequent outlier. Hence, field no. 3 was excluded from all data sets. Within each experiment, the means of each feature output of the wells treated with 15 μM sodium arsenite (with 0.125% DMSO), ie, column 12 of plates 2, 3, 4, and 5, were normalized to those of plate 1. The individual well values of each feature output on a plate were then transformed against the normalized mean feature outputs of the 15 μM arsenite-treated wells on that plate to account for interplate differences. Statistical differences were calculated from normalized values by 1-way ANOVA (with Dunnett's post hoc comparison of treatment groups to DMSO vehicle control).

Immunofluorescent imaging of Tdp-43 in primary neuronal culture. Primary hippocampal neurons were isolated from P0 CD1 pups and cultured in neurobasal medium (Gibco, 21103049) supplemented with 2% B-27 (Gibco, 17504044), 200 μM L-glutamine (Gibco, 25030081), and PenStrep. Animals were housed and treated according to Boston University School of Medicine IACUC-approved protocols. Hippocampal neurons were plated at 1×10^5 cells/well onto nitric acid-washed, poly-D-Lysine-coated 12 mm coverslips in 24 well plates then maintained 14 days in vitro (DIV) before treating in quadruplicate for 6 h with lead (II) acetate trihydrate (at 0.174, 0.521, 1.56, and 4.69 μM; Sigma) or methyl mercuric (II) chloride (at 0.058, 0.174, 0.521, and 1.56 μM). Previous studies of neuronal death have used lead treatment in the range of 0.2–2 μM and methyl mercury in the range of 10 nM–1 μM (Engstrom *et al.*, 2015; Fujimura and Usuki, 2012). After treatment, hippocampal neurons were then washed in PBS, fixed in 4% PFA in PBS, permeabilized with PBS w/0.5% Tween 20, blocked with 10% normal donkey serum (Sigma) in PBS, and immunostained overnight with 1:400 (rabbit) anti-Tdp-43 (ProteinTech; 12983-1-AP) and 1:200 (chicken) anti-Map2 (Aves labs; MAP). Images (4 independent experiments per treatment, 10 images per experimental coverslip, ∼3 neurons per ROI = approx. 120 neurons per treatment group) were acquired at 63× as z-stacks on a Zeiss AxioObserver A1 with equal exposures for all treatment groups, deconvolved then compressed into maximum intensity projection images (Zen, Zeiss). Tdp-43 granules were detected in Bitplane (Imaris) using a masking algorithm that identifies neuronal cells (by Map2), neuronal nuclei (based on size, sphericity, and an intensity threshold for Tdp-43 and DAPI signal within Map2 cells) and nuclear Tdp-43 granules (based on an intensity threshold for Tdp-43 and an estimated diameter of 0.45 μm). Outliers were removed in GraphPad Prism by ROUT (Q = 0.1%). Statistical analyses were performed as described above.

Splicing of sortilin1 *exon 17b as an assay of Tdp-43 function.* Primary CD1 cortical neurons were plated at 2×10^6 cells/well onto PDL-coated 6 well plates and maintained in culture until commencing treatment on DIV7. These neurons were treated ($n = 6$) every 48 h with 0.521 or 1.56 μM lead (II) acetate trihydrate. At DIV14, total RNA was extracted by RNeasy minikit (Qiagen), quantified and reverse transcribed by High-Capacity cDNA Reverse Transcription Kit (Thermo) before qPCR analysis using SYBR Green master mix (Bio-Rad). Relative levels of total *sortilin 1* (*Sort1*), *Tardbp*, and *Actb* were quantified and normalized to the means of untreated group. Alternate splicing of *Sort1* was assessed as reported previously (Prudencio *et al.*, 2012) using qPCR primer sets to quantify the relative levels of $Sort1_{WT}$ transcripts (with exclusion of exon 17b) and $Sort1_{+17b}$ transcripts. Primer sets are reported in Supplementary Table 2.

Liquid-liquid phase separation of TDP-43. Recombinant TDP-43 was produced as described previously (Carlomagno *et al.*, 2014). Briefly, human TDP-43 was produced in bacteria with expression induced with IPTG at 16°C. Pelleted bacteria were lysed and clarified, and proteins were precipitated in 15% ammonium sulfate solution. Precipitated proteins were resuspended, dialyzed, and clarified before confirming purity by SDS-PAGE/Coomassie. Phase separation of 5 μM TDP-43 was performed in 10 mM HEPES, pH 7.4, 100 mM NaCl, 20 ng/μl total murine brain RNA and induced with addition of 1% polyethylene glycol (PEG)-8000. 0.0025% of 1 micron Polybead® Carboxylate inert polystyrene microspheres (Polysciences) were added to LLPS reactions to aid sample focusing. Reactions were performed at 24°C for 2 h in triplicate reactions with 10, 20, 40, 80, 160, 320, and 640 μM lead (II) acetate trihydrate, nickel (II) sulfate, zinc (II) sulfate, or cobalt (II) chloride. Droplet formation was detected by differential interference contrast at 63× in 3 μl reactions in coverslipped slide microchambers created from SecureSeal spacers (Grace Bio-Labs). TDP-43 droplets were counted in ImageJ(Fiji) (Schindelin *et al.*, 2012): (1) Plugins>Filters>Enhance local contrast; (2) Process>Enhance contrast: normalize histogram; (3) Image>Type > 8-bit, Image>Color>Edit LUT: ICA, Image>Type>RGB, Image>Type > 8-bit; (4) Plugins>Filters>Enhance local contrast; (5) Process>Filters>Gaussian blur: 7; (6) Image>Adjust>Threshold: Triangle method; and (7) Analyze>Analyze particles. Droplet count was quantified as percentage of image area covered by droplets.

TDP-43:: GFP solubility in lead-exposed PC12 cells. PC12 cells were cultured and induced as described above. For TDP-43 solubility and expression studies, 5×10^5 induced PC12 cells/well were plated to collagen-coated 6-well plates (Gibco, A11428-01). The following day (DIV1), cells were treated in triplicate with lead (II) acetate trihydrate at concentrations of 0.174, 0.521, 1.56, and 4.69 μM by adding stock solutions directly to the 2 ml culture media of each well. The treatment was reapplied on DIV3 and DIV5 by aspirating, replacing induction media (containing no doxycycline), and adding compound. Cells were harvested on DIV6 by washing twice with PBS, scraping the cells into PBS, pelleting (800 rcf for 2 min) then lysed by sonication in RIPA buffer. Sample concentrations were determined by BCA assay. Blotting of total lysates and RIPA solubility of TDP-43:: GFP was performed as described previously (Ash *et al.*, 2017). Blots were incubated with the following antibodies: 1:1000 anti-phospho-S409/410 TDP-43 (a gift from Leonard Petrucelli, Mayo Clinic, Rb3655), 1:2000 anti-GFP (Sigma; G1544), 1:2000 anti-TDP-43 (ProteinTech; 12892–1-AP); and 1:10000 anti-Actin (Millipore; MAB1501). Blots were imaged using HRP-conjugated secondary antibodies (Jackson) activated with Pierce ECL chemiluminescent substrates (Thermo Fisher) and a ChemiDoc XRS+ Imager (BioRad). Band densitometries were assessed using Image Lab Software (Bio-Rad) and GraphPad Prism was used to perform ANOVA statistical analyses with Dunnett's multiple comparison test against untreated controls.

In vivo methyl mercury exposure and analysis of murine cortical tissue. Nine-month-old, male BALB/c mice were purchased from Envigo Laboratories (Indianapolis, Indiana) and individually housed in a temperature- and humidity-controlled AAALAC-accredited animal facility. All procedures were approved by the

Auburn University Institutional Animal Care and Use Committee. Upon arrival, mice were exposed to 0 or 5 ppm MeHg as methyl mercuric (II) chloride dissolved in drinking water. Mice had free access to water and were maintained at approximately 25 (±1) g body mass via daily feedings of 3.0 (±1) g chow. Mice were food restricted to motivate responding in behavioral experiments and to maintain healthy body mass (for details, see Shen *et al.*, 2016). After 42 weeks of exposure (at approximately 18 months of age), mice were euthanized via decapitation and the whole brain was extracted, frozen, and stored for later analysis. A total of ~60 mg of frozen cortical tissue was lysed by bead mill (Thermo) homogenization in 1 ml Qiazol reagent (Qiagen) then the RNA was extracted following the Lipid tissue RNeasy minikit protocol (Qiagen). qPCR on reverse-transcribed total RNA was performed as described above. A total of ~100 mg of frozen cortical tissue was lysed by bead mill (Thermo) homogenization in Tris-EDTA buffer (10 mM Tris pH8; 1 mM EDTA; 1 mM PMSF; 1× HALT PIC, and PhosSTOP [Roche]). Sample concentrations were determined by BCA assay. Solubility of murine Tdp-43 was assayed as described previously (Neumann *et al.*, 2006). Briefly, equal amounts of cortical lysates were sequentially extracted by ultracentrifugation in buffers containing increasing detergent strengths. The final pellet is the product of insolubility in 1% sarkosyl/500 mM NaCl centrifuged at 180 000 rcf for 30 min then re-suspended in 8 M urea buffer. Total TE lysates, sarkosyl soluble, and sarkosyl insoluble fractions were then blotted as described above and immunolabelled using 1:2000 anti-TDP-43 (ProteinTech; 12892–1-AP) and 1:10 000 anti-Actin (Millipore; MAB1501). Band densitometries were assessed using Image Lab Software (BioRad) and unpaired two-tailed *t* tests performed in GraphPad Prism.

RESULTS

Screening for Neurotoxicants in an Inducible TDP-43::GFP Cell Line

We previously generated a rat PC12 cell line that stably expresses Tet-off-inducible wild-type human TDP-43::GFP that forms inclusions of TDP-43:: GFP upon treatment with sodium arsenite (Supplementary Figure 2) (Boyd *et al.*, 2014). Using this cell line, the 91 compound "NeuroTox" plate (Behl *et al.*, 2018) was screened by a blinded researcher to identify putative neurotoxins that result in aggregation of TDP-43, the loss of diffuse nuclear TDP-43, and cell death. A number of compounds were cytotoxic leading to dose-dependent cell death, other toxicants (often at the highest concentration) triggered statistically significant but biologically small effects to the TDP-43 (chemical list and screening results in Supplementary Table 1 and Figs. 1A–E). Four toxicants robustly increased the percentage of cells with TDP-43:: GFP aggregates or the ratio of cells with TDP-43:: GFP aggregates/diffuse TDP-43:: GFP (Figure 1A). Lead (II) acetate trihydrate (Figure 1B, compound F2) caused TDP-43:: GFP to aggregate (DMSO, $\bar{x} = 15.3\%$, ±2.12 SEM, of cells; lead (II) acetate trihydrate maximal affect at 25 μM, $\bar{x} = 38.8\%$, ±4.33 SEM, $p < .0001$) without substantially affecting the percentage of cells with diffuse TDP-43:: GFP or causing significant cell death. Methyl mercuric (II) chloride treatment caused significant aggregation of TDP-43:: GFP with concurrent reduction in the percentage of cells with diffuse TDP-43:: GFP (DMSO aggregates/diffuse ratio, $\bar{x} = 28.9$, ±3.41 SEM; methyl mercuric (II) chloride maximal affect at 6.25 μM, $\bar{x} = 126$, ±23.4 SEM, $p < .0001$). Treatment with methyl mercuric (II) chloride at the higher doses of 25 and 100 μM caused substantial cell death ($p < .05$ vs cell count with DMSO). Unknown to the researcher who completed the screen, methyl mercuric (II) chloride was placed on the NeuroTox plate twice (Figure 1B, compounds F5 and H5) and generated similar results, indicating the accuracy of the PC12 stable cell line as a means to observe neurotoxin effects on TDP-43. Bis(tributyltin)oxide (Figure 1B, compound C10) treatment similarly increased the ratio of cells with aggregates versus diffuse TDP-43:: GFP (maximal affect at 1.56 μM, $\bar{x} = 206$, ±53.0 SEM, $p < .0001$) with significant cell death triggered by the highest doses of 1.56 and 6.25 μM. Colchicine (Figure 1B, compound D8) increased the levels of both aggregated and diffuse TDP-43:: GFP at all concentrations without generating cytotoxicity. While a number of the putative developmental neurotoxins screened had some affect on cell survival and TDP-43 distribution, the identification that lead-, mercury- and tin-based compounds induce aggressive aggregation of TDP-43 is particularly interesting as exposure to heavy metal compounds have been linked with increased risk of ALS (Beghi *et al.*, 2006).

Lead and Methyl Mercury Trigger Formation of Endogenous Tdp-43 Inclusions

To assess whether heavy metal compounds affect endogenous TDP-43 in neuronal cells, we cultured primary hippocampal neurons from P0 CD1 pups to better reflect the biology of the central nervous system. Previous studies from our laboratory show that hippocampal neurons reflect the biology of ALS. They exhibit abundant TDP-43 in the processes, dendritic TDP-43 granules whose size and movement respond to mutations in TDP-43, develop strong cytoplasmic aggregates of TDP-43 upon exposure to stress, and have glutamate receptors (Liu-Yesucevitz *et al.*, 2014). Importantly, TDP-43 pathology occurs in the hippocampus and neocortex in ALS and some ALS patients develop overt cognitive decline (Brettschneider *et al.*, 2013; Goldstein and Abrahams, 2013). Neurons were grown for 14 days then exposed for 6 h to lead (II) acetate trihydrate (at 0.174, 0.521, 1.56, and 4.69 μM) or methyl mercuric (II) chloride (at 0.058, 0.174, 0.521, and 1.56 μM). Both compounds caused endogenous Tdp-43 to form nuclear granules, which were detected by immunofluorescence and quantified using a masking algorithm (Figure 2A, Supplementary Figure 3A). Exposure to lead (II) acetate trihydrate triggered formation of nuclear Tdp-43 inclusions in a biphasic manner (Figure 2B). A total of 0.174 μM lead produced ~4× fold more granules per neuronal nuclei compared with the vehicle, 0.571 μM lead produced a ~2.5× fold increase, 1.56 μM lead produced a ~5× fold increase, and 4.69 μM lead produced a ~3.5× fold increase (DMSO granules/nuclei, $\bar{x} = 0.57$, ±0.19 SEM; lead 0.174 μM, $\bar{x} = 2.52$, ±0.63 SEM, $p < .01$; lead 0.521 μM, $\bar{x} = 1.46$, ±0.27 SEM, ns; lead 1.56 μM, $\bar{x} = 3.00$, ±0.54 SEM, $p < .001$; lead 4.69 μM, $\bar{x} = 2.00$, ±0.46 SEM, $p < .05$). These data suggest that lead compounds employ different molecular pathways to induce Tdp-43 accumulation at different concentrations. Methyl mercuric (II) chloride triggered formation of nuclear Tdp-43 inclusions in a dose-dependent fashion, gaining significance at the 0.521 μM dose with ~4× fold granules per neuronal nuclei compared with the vehicle control (Figure 2B; DMSO granules/nuclei, $\bar{x} = 0.57$, ±0.19 SEM, mercury, $\bar{x} = 2.43$, ±0.43 SEM, $p < .01$). In Supplementary Figure 3B, the frequency with which neurons develop a set number of granules per nuclei is plotted. At those doses of both lead and methyl mercury that significantly increase the mean number of inclusions per neuron, both the frequency in the number of neurons with nuclear inclusions and the number of inclusions in those nuclei increases. The discovery that lead and methyl mercury cause formation of Tdp-43 inclusions in neurons is hugely important because it is the first demonstration of a putative molecular

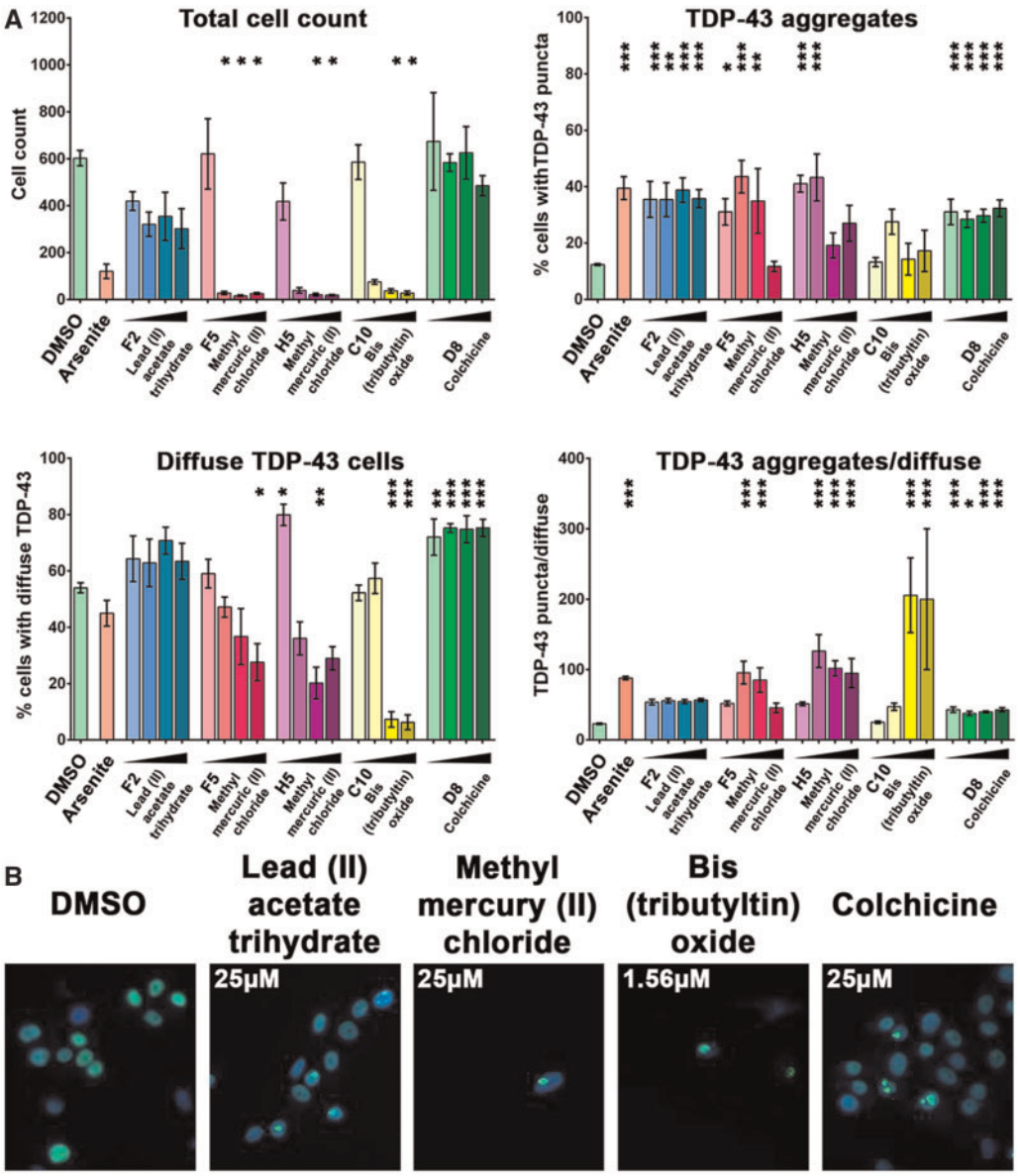

Figure 1. A screen of neurotoxins in inducible stably expressing cells reveals heavy metals trigger formation of nuclear TDP-43:: GFP inclusions. PC12 cells expressing TDP-43:: GFP were screened against developmental neurotoxins in the NTP HTS NeuroTox 91 Plate (Chemical list, Supplementary Table 1). High-content imaging was used to quantify cell count, number of cells with diffuse TDP-43:: GFP and number of cells with nuclear TDP-43:: GFP inclusions (full screening results in Supplementary Figs. 1A–E). A, Four compounds were found to induce formation of TDP-43 inclusions: lead (II) acetate trihydrate (compound ID: **F2**), methyl mercuric (II) chloride (**F5, H5**), colchicine (**D8**) (concentrations: 1.56, 6.25, 25, and 100 μM) and Bis(tributyltin)oxide (**C10**) (concentrations: 0.1, 0.39, 1.56, and 6.25 μM). $N = 4$; mean ±SEM; ANOVA w/Dunnett's multiple comparison test, $^{*}p < .05$, $^{**}p < .01$, $^{***}p < .01$. B, Representative images of merged GFP and DAPI signals show cells with diffuse nuclear TDP-43:: GFP upon DMSO (vehicle control) treatment and nuclear TDP-43:: GFP inclusions upon exposure to lead (II) acetate trihydrate, methyl mercuric (II) chloride, bis(tributyltin)oxide, and colchicine (at concentrations shown). Representative images of positive control (2 μM arsenite), uninduced PC12 cells, and different compound doses are shown in Supplementary Figure 2.

mechanism mediating the linkage between exposure to heavy metals and ALS.

Lead Treatment of Neurons Inhibits Tdp-43 Splicing of Sortilin 1 *Exon 17b*

Sortillin 1 (*Sort1*) is a known target of alternative splicing mediated by TDP-43, with knockdown or deletion of TDP-43 increasing the inclusion of exon 17b (Afroz *et al.*, 2017; Polymenidou *et al.*, 2011; Prudencio *et al.*, 2012). We hypothesized that lead-induced perturbation of nuclear Tdp-43 would alter its function resulting in dysregulation of splicing. Primary cortical neurons were treated every 48 h for 7 days with 0.521 or 1.56 μM lead (II) acetate trihydrate (Pb). qPCR observation of the ratio of *sortilin 1* transcripts containing exon 17b ($Sort1_{+Ex17b}$) over *sortilin 1* wild-type transcripts ($Sort1_{WT}$; excluding Ex17b) shows that lead significantly reduces inclusion of exon 17b (Figure 2C; untreated ratio, $\bar{x} = 1.00$, ±0.065 SEM, 1.56 μM Pb, $\bar{x} = 0.793$, ±0.024 SEM, $p < .05$). Lead treatment also produced a significant increase in the transcript levels of Tdp-43 (*Tardbp*; Figure 2D; untreated, $\bar{x} = 1.00$, ±0.049 SEM, 1.56 μM Pb, $\bar{x} = 1.22$, ±0.020 SEM, $p < .05$) and in the total levels of *Sort1* transcript (Supplementary Figure 4; untreated, $\bar{x} = 1.00$, ±0.045 SEM, 1.56 μM Pb, $\bar{x} = 1.17$, ±0.038 SEM, $p < .05$). While the effect at the 0.521 μM dose was not significant, the trend observed was similar to that with the higher

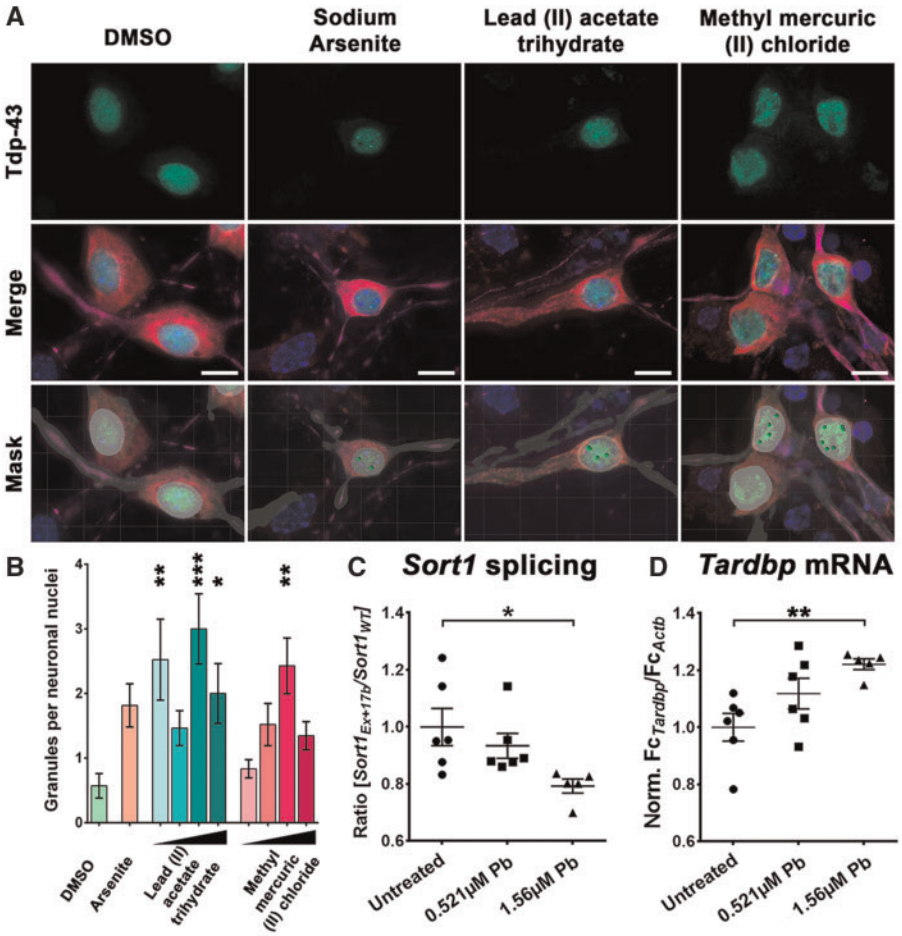

Figure 2. Exposure to lead and methyl mercury triggers formation of neuronal nuclear inclusions of endogenous Tdp-43. A, Primary hippocampal neurons (DIV14) exposed for 6 h to lead (II) acetate trihydrate and methyl mercuric (II) chloride develop nuclear inclusions of endogenous Tdp-43. Neurons were immunolabelled with antibodies to MAP2 (magenta) and Tdp-43 (green) and nuclei were counterstained with DAPI (blue). Shown are representative images of neurons treated with 2 μM sodium arsenite, 4.69 μM lead (II) acetate trihydrate, and 1.56 μM methyl mercuric (II) chloride. Secondary only controls show no immunolabel (Supplementary Figure 3). A masking algorithm (Imaris, Bitplane) was used to detect and quantify inclusions per neuronal nuclear. B, Lead (II) acetate trihydrate concentrations: 0.174, 0.521, 1.56, and 4.69 μM; methyl mercuric (II) chloride concentrations: 0.058, 0.174, 0.521, and 1.56 μM. $N = 4$; mean ± SEM; ANOVA w/Dunnett's multiple comparison test versus DMSO control, $^{*}p < 0.05$, $^{**}p < 0.01$, $^{***}p < 0.01$. C, Lead at 1.56 μM effects the alternative splicing function of Tdp-43 leading to reduced ratio of inclusion of *Sort1* exon 17b compared with wild-type *Sort1* transcripts. This negatively correlates (Supplementary Figure 4E; slope = −0.65 ± 0.21, $R^2 = 0.39$, $p = .0074$) with an increase in transcript levels of Tdp-43 (*Tardbp*) (D) upon lead treatment. $N = 6$; mean ±SEM; ANOVA w/Dunnett's multiple comparison test, $^{*}p < .05$, $^{**}p < .01$.

dose. The decrease in inclusion of *Sort1* exon 17b suggests that the increased nuclear accumulation of total Tdp-43 that is associated with exposure to Pb increases splicing activity mediated by Tdp-43. Multiple studies have shown that both increases and decreases in Tdp-43 levels are toxic (Tsao *et al.*, 2012).

Lead Accelerates Phase Separation of TDP-43

RBPs regulate many aspects of RNA metabolism through RNA binding via the RNA binding domains and through reversible self-assembly and LLPS (formation of liquid droplets) via intrinsically disordered regions (IDRs). LLPS has been modeled for multiple RBPs in vitro, including TDP-43, using recombinant purified proteins (Wang *et al.*, 2018). Protein, salt, and crowding reagent concentrations modulate the kinetics of TDP-43 LLPS (Wang *et al.*, 2018). Phase separation of 5 μM TDP-43 did not occur over a 2 h experiment using 100 mM NaCl, 1% PEG (a crowding reagent), and 20 ng/μl total murine brain RNA. However, addition of lead (II) acetate trihydrate to the reaction mix promoted TDP-43 LLPS in a dose-dependent manner (Figure 3A; mask in Supplementary Figure 5A) with an EC_{50} of 160 μM (Figure 3B; 95% CI 150.5 to 169.4, $R^2 = 0.887$; 5 images each from 3 independent experiments). Interestingly, at low concentrations of lead, TDP-43 formed small single droplets (arrows in Figure 3A), while at higher concentrations of lead, TDP-43 phase separates into large amorphous consolidates (asterisk in Figure 3A). Neither nickel (II) sulfate nor cobalt (II) chloride induced TDP-43 LLPS at the highest concentration. However, zinc (II) sulfate triggered robust phase separation in a dose-dependent manner with a lower EC_{50} of 79.3 μM (Supplementary Figs. 5B and 5C).

Lead Exposure Results in Accumulation of Insoluble TDP-43

To address whether lead produces a similar change in solubility of TDP-43 in cells, PC12 cells were induced to express TDP-43:: GFP and then exposed to lead (II) acetate trihydrate for 6 days in triplicate at concentrations of 0.174, 0.521, 1.56, and 4.69 μM. The solubility of TDP-43:: GFP in RIPA buffer was then assessed by ultracentrifugation and immunoblotting of the RIPA insoluble (Figure 3C), RIPA soluble (Figure 3D), and total RIPA lysate (Figure 3E). At the lower concentrations of lead (0.174 and 0.521 μM), the total levels of TDP-43:: GFP increased significantly (Figs. 3E and 3F; untreated, $\bar{x} = 1.00$, ±0.073 SEM, 0.174 μM Pb,

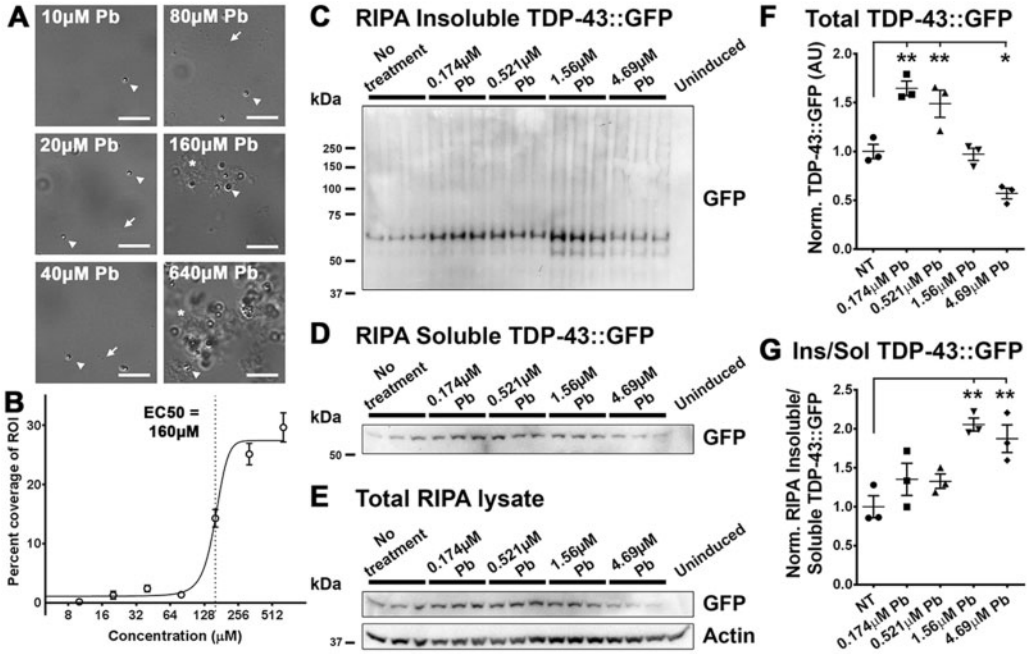

Figure 3. Lead triggers phase separation of TDP-43 and decreases its solubility. A, Purified TDP-43 LLPS in vitro is facilitated by lead (II) acetate trihydrate (Pb) in a dose-dependent manner. Representative 63× DIC images. Arrows: examples of single TDP-43 droplets. Asterisk: examples of amorphous TDP-43 consolidates. Arrowheads: high-contrast, inert 1 micron polystyrene microspheres added to aid sample focusing. Scale bar = 10 μm. B, LLPS was quantified using an ImageJ algorithm as percentage of ROI covered by droplets. Points at mean, with error bars at SEM, were fit by nonlinear regression analysis (line) and the LogEC50 calculated as 160 μM (dotted line). Induced PC12 cells accumulate insoluble TDP-43:: GFP upon treatment with lead (Pb). Immunoblots of RIPA insoluble (C), RIPA soluble (D) and total RIPA lysate (E) were probed with anti-GFP antibodies ($N = 3$). F, Densitometric analysis of total TDP-43:: GFP/Actin bands (from panel E) show an increase in TDP-43:: GFP in response to 0.174 and 0.521 μM lead but an decrease in response to 4.69 μM lead. G, At 1.56 and 4.69 μM concentrations, lead significantly increases the ratio of insoluble TDP-43:: GFP to soluble TDP-43:: GFP. $N = 3$; mean ± SEM; ANOVA w/Dunnett's multiple comparison test, $^{*}p < .05$, $^{**}p < .01$. AU: arbitrary units. Predicted molecular weight of TDP-43:: GFP ~70 kDa. Uninduced PC12 cells express no TDP-43:: GFP.

$\bar{x} = 1.65$, ±0.074 SEM, 0.521 μM Pb, $\bar{x} = 1.49$, ±0.193 SEM, $p < .01$). At the highest concentration, 4.69 μM, lead treatments resulted in significantly reduced TDP-43:: GFP (4.69 μM Pb, $\bar{x} = 0.57$, ±0.054 SEM, $p < .05$), though this effect was coupled with substantial cell loss and may reflect death of high TDP-43:: GFP expressing cells. Interestingly, exposure to lead robustly decreased the solubility of TDP-43:: GFP. At concentrations of 0.174, 0.521, and 1.56 μM a significant increase in the RIPA insoluble TDP-43:: GFP was detected (Supplementary Figure 6C). However, at the lower doses of 0.174 and 0.521 μM, this may be due in part to the increase in levels of total TDP-43:: GFP, as the levels of RIPA soluble TDP-43:: GFP also increases at these lower doses (Figure 3D). When the ratio of insoluble TDP-43:: GFP over soluble TDP-43:: GFP is compared (Figure 3G), it reveals that exposure to the higher doses of 1.56 and 4.69 μM lead triggers the accumulation of insoluble TDP-43:: GFP (untreated, $\bar{x} = 1.00$, ±0.140 SEM, 1.56 μM Pb, $\bar{x} = 2.06$, ±0.083 SEM, 4.69 μM Pb, $\bar{x} = 1.87$, ±0.179 SEM, $p < .01$). Insoluble TDP-43 pathology in ALS is hyperphosphorylated with consistent phosphorylation of S409/410 (Neumann *et al.*, 2009). Using an antibody that detects pS409/410 TDP-43 (Chew *et al.*, 2015), we observed a significant accumulation of insoluble phosphorylated TDP-43:: GFP in PC12 cells exposed to 1.56 and 4.69 μM lead (Supplementary Figs. 6B and 6D).

Systemic Administration of Methyl Mercury Results in Accumulation of Insoluble Tdp-43

We sought to study whether systemic exposure to methyl mercuric (II) chloride in vivo disrupted TDP-43 homeostasis in the brain. 9-month old BALB/c mice were exposed to 0 ppm (no treatment) or 5 ppm methyl mercuric (II) chloride in water provided ad libitum for 42 weeks (Shen *et al.*, 2016). Solubility of Tdp-43 in cortical tissue was assayed by biochemical fraction methods previously used to detect insoluble TDP-43 in neurodegenerative disease (Neumann *et al.*, 2006). Immunoblots of sarkosyl insoluble material shows that systemic exposure to 5 ppm MeHg results in $a > 2.5$-fold increase in insoluble monomeric Tdp-43 (Figs. 4A and 4C; no treatment, $\bar{x} = 1.00$, ± 0.127 SEM, 5 ppm MeHg, $\bar{x} = 2.52$, ±0.379 SEM, $p < .05$) and high molecular weight Tdp-43 (Figure 4D; no treatment, $\bar{x} = 1.00$, ±0.159 SEM, 5 ppm MeHg, $\bar{x} = 3.21$, ±0.592 SEM, $p < .05$). In the total lysate, Tdp-43 was slightly elevated at both the protein (Figure 4B, Supplementary Figure 7A) and transcript level (Supplementary Figure 7B), but this difference was only significant at the trend level ($p = .099$ and .129, respectively). Similar to the effect observed in primary neuronal cultures treated with lead, 5 ppm MeHg exposure resulted in a significant reduction in inclusion of alternatively spliced exon 17b in cortical *sortilin 1* transcripts (Supplementary Figs. 7C–F). This data, together with that collected from lead treatment of PC12 cells, provide strong evidence that the heavy metals lead and methyl mercury trigger accumulation of insoluble phosphorylated TDP-43.

DISCUSSION

Epidemiological studies suggest that environmental toxicants including heavy metals (such as lead, mercury, and selenium) are risk factors for ALS (reviewed in Trojsi *et al.*, 2013), but the mechanism underlying the risk is unknown. The sensitivity of individual studies is sometimes confounded by difficulties in

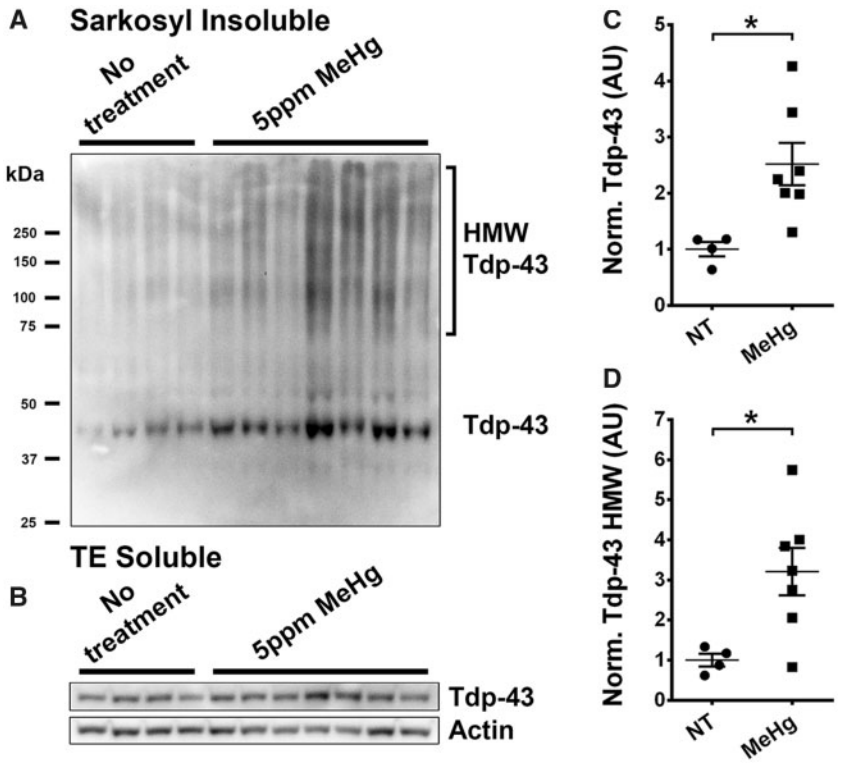

Figure 4. Methyl mercury exposure results in cortical accumulation of insoluble Tdp-43. Cortical tissue from mice exposed, by ingestion, to 0 ppm (no treatment, $N = 4$) and 5 ppm methyl mercuric (II) chloride (MeHg, $N = 7$) was fractionated by solubility. The sarkosyl insoluble (A) and total lysate (B) (TE: Tris-EDTA) fractions were immunoblotted and probed for endogenous Tdp-43. Upon systemic MeHg exposure, sarkosyl insoluble Tdp-43 (C) and high molecular weight (HMW) Tdp-43 (D) is significantly increased. Mean ±SEM; unpaired two-tailed *t* test, $^{*}p < .05$. AU: arbitrary units.

correlating degree of metal exposure to disease onset and severity, which means meta-analyses can be more informative than individual studies. Indeed, a meta-analysis of published works estimated an odds of developing ALS to be 1.81 in individuals with chronic occupational exposure to lead (odds ratio of 1.87 when reports of lead exposure are combined with reports of heavy metal exposure) (Wang *et al.*, 2014). Elevated levels of heavy metals have been documented in the blood (Garzillo *et al.*, 2014) and CSF (Vinceti *et al.*, 2013, 2017) of ALS-affected patients. In ALS patient CSF, median ^{208}Pb (lead) concentrations were detected at 2.71 μg/l (or ~10 nM) and for ^{200}Hg (mercury) at 0.065 μg/l (or ~0.325 nM) (Roos *et al.*, 2013) but troublingly, the Center for Disease Control recognizes "blood lead level of concern" at the higher level of >10 μg/dl (or 0.482 μM). These epidemiological studies complement the current work, in which lead (Pb) and methyl mercury (MeHg) were identified through a blinded, unbiased screen of common toxicants and provides important support for the hypothesis that Pb and MeHg contribute to the risk of ALS by acting as inducers of TDP-43 inclusions. The ability to use high throughput screening to gain mechanistic insights and identify putative toxicants for particular diseases is incredibly important. This could be a valuable approach to identify other neurodegenerative disease-causing toxicants and the potential mechanisms of action of these toxicants.

Disruption of TDP-43 homeostasis, either increasing or decreasing its activity, is associated with motor neuron dysfunction (Lagier-Tourenne *et al.*, 2010; Tsao *et al.*, 2012). Decreased nuclear TDP-43, which in disease occurs concurrently with translocation and cytoplasmic aggregation, is classically associated with loss of splicing regulation. Studies show that the loss of TDP-43 activity associated with increased aggregation is deleterious, but point mutations in the C-terminus of TDP-43 that increase splicing-suppressive activity can also result in motor neuron loss and neuromuscular deficits (Fratta *et al.*, 2018). In the current study, we observe that heavy metals increased formation of nuclear inclusions of TDP-43, increased total levels of TDP-43 and increased TDP-43-mediated splicing activity, thereby suppressing splicing events in the *sortillin 1* (*Sort1*) gene. Heavy metals also increased levels of aggregated TDP-43, which is thought to be physiologically inactive but is strongly associated with neurodegeneration. Our results suggest that TDP-43 nuclear splicing activity is more sensitive to changes in total TDP-43 levels than the accumulation of aggregated TDP-43. It is important to note that changes in *Sort1* splicing activity in response to heavy metal exposure could also reflect actions on other nuclear components unrelated to TDP-43.

There is currently immense interest in the subject of LLPS because it represents a novel mechanism of protein association that appears to be of fundamental importance to the field of cell biology (Li *et al.*, 2018; Molliex *et al.*, 2015; Shin and Brangwynne, 2017; Wang *et al.*, 2018). Given this context, our observation that lead increases LLPS of TDP-43 in vitro is particularly significant. We hypothesize that toxic divalent metals increase TDP-43 oligomerization to effectively move TDP-43 along the phase separation curve into a region of increased droplet stability (nuclear bodies) (Shin and Brangwynne, 2017). There is precedence for perturbation of TDP-43 biology, as zinc binding to a segment of TDP-43 corresponding to the RNA recognition motifs cause TDP-43 to form aggregates in vitro (Garnier *et al.*, 2017), and the treatment of cultured mammalian cells with zinc triggers formation of TDP-43 granules (Caragounis *et al.*, 2010). Thus, other heavy divalent metal cations (lead, mercury, tin, and selenium)

might induce TDP-43 dysfunction in a similar manner to zinc. However, neither of the studies of zinc investigated LLPS. The construction of many essential biological structures is achieved through LLPS, such as the nucleolus, RNA granules, and the nuclear pore. As such, LLPS contributes to many critical cellular functions, including RNA splicing, RNA transport, RNA translation, and ribosomal genesis (Shin and Brangwynne, 2017). Hence, our observation that metals alter LLPS suggests a potentially novel mechanism through which metal toxicants might cause cellular dysfunction and human disease.

Many fundamental questions remain to be answered by future studies. One key question is whether motor neurons are selectively vulnerable to metal toxicants, as well as other toxicants linked to ALS. The question of selective vulnerability is key to the study of virtually every neurodegenerative disease because most disease-related proteins are present throughout the brain (and often throughout the body), yet the pathology begins in a cell-type selective manner. The availability of reagents such as induced pluripotent stem cells and single cell sequencing are beginning to provide the tools that might answer such questions of cell selectivity, but is beyond the scope of the current study. Another important question is the relationship between LLPS and disease pathology. Some studies suggest that insoluble aggregates, resembling those observed in disease, can evolve directly from the phase separation process (Molliex *et al.*, 2015; Patel *et al.*, 2015). A recent study suggests that transient phase separation of TDP-43 protects against disease-associated phosphorylation, but that under long-term stress aggregates of phosphorylated TDP-43 form (McGurk *et al.*, 2018). We observe modulation of TDP-43 LLPS in vitro and cultured neurons by exposure to metal toxicants and formation of insoluble aggregates after extended exposure. This raises the possibility that metal toxicants increase the risk of ALS by prolonging neuronal LLPS of TDP-43, with consequent disruption of TDP-43 function and formation of insoluble aggregates.

The work presented here reveals that heavy metals trigger formation of nuclear TDP-43 inclusions and perturb its RNA metabolic functions. These results provide novel evidence of a direct mechanistic connection between heavy metals, a commonly cited environmental risk of ALS, and molecular changes in TDP-43, the primary pathological protein of ALS. This finding warrants further study of the molecular mechanisms by which heavy metals drive TDP-43 pathology and of the epidemiological connection between heavy metal exposure and ALS. It also supports the use of the inducible TDP-43:: GFP PC12 cell line as an accurate platform for environmental toxicants and other modifiers that play a role in the etiology of ALS and hence should be considered as a part of a larger battery to screen for neurotoxicants. These discoveries will provide further understanding of the disease mechanisms of ALS and deliver significant benefits for public health.

SUPPLEMENTARY DATA

Supplementary data are available at *Toxicological Sciences* online.

AUTHORS CONTRIBUTIONS

PEAA conceived, performed, and analyzed experiments, and wrote the original draft. UD conceived, performed and analyzed experiments. SB, SL, and LFAAM performed experiments. YC provided essential reagents. MK designed ImageJ algorithm. SRB and MCN conducted in vivo MeHg exposures. DHS provided expertise. BW conceived, analyzed, edited, supervised, and provided funding for the project.

ACKNOWLEDGMENTS

Polyclonal antibody Rb3655 anti-PS409/410 TDP-43 was kindly provided by Leonard Petrucelli, Mayo Clinic.

FUNDING

UD: UGC-Raman Fellowship from Government of India. BW: NIH (ES020395, AG050471, NS089544, AG056318) BrightFocus Foundation, Alzheimer Association, Cure Alzheimer's Fund, and the Thome Memorial Foundation.

REFERENCES

Afroz, T., Hock, E.-M., Ernst, P., Foglieni, C., Jambeau, M., Gilhespy, L. A. B., Laferriere, F., Maniecka, Z., Plückthun, A., and Mittl, P. (2017). Functional and dynamic polymerization of the ALS-linked protein TDP-43 antagonizes its pathologic aggregation. *Nat. Commun.* **8**, 45.

Arai, T., Hasegawa, M., Akiyama, H., Ikeda, K., Nonaka, T., Mori, H., Mann, D., Tsuchiya, K., Yoshida, M., Hashizume, Y., *et al.* (2006). TDP-43 is a component of ubiquitin-positive tau-negative inclusions in frontotemporal lobar degeneration and amyotrophic lateral sclerosis. *Biochem. Biophys. Res. Commun.* **351**, 602–611.

Aschner, M., Ceccatelli, S., Daneshian, M., Fritsche, E., Hasiwa, N., Hartung, T., Hogberg, H. T., Leist, M., Li, A., Mundi, W. R., *et al.* (2017). Reference compounds for alternative test methods to indicate developmental neurotoxicity (DNT) potential of chemicals: Example lists and criteria for their selection and use. *Altex* **34**, 49–74.

Ash, P. E. A., Stanford, E. A., Al Abdulatif, A., Ramirez-Cardenas, A., Ballance, H. I., Boudeau, S., Jeh, A., Murithi, J. M., Tripodis, Y., Murphy, G. J., *et al.* (2017). Dioxins and related environmental contaminants increase TDP-43 levels. *Mol. Neurodegener.* **12**, 35.

Bal-Price, A., Coecke, S., Costa, L., Crofton, K. M., Fritsche, E., Goldberg, A., Grandjean, P., Lein, P. J., Li, A., Lucchini, R., *et al.* (2012). Advancing the science of developmental neurotoxicity (DNT): Testing for better safety evaluation. *ALTEX* **29**, 202–215.

Beghi, E., Logroscino, G., Chiò, A., Hardiman, O., Mitchell, D., Swingler, R., and Traynor, B. J. (2006). The epidemiology of ALS and the role of population-based registries. *Biochim. Biophys. Acta* **1762**, 1150–1157.

Behl, M., Ryan, K., Hsieh, J.-H., Parham, F., Shapiro, A. J., Collins, B. J., Birnbaum, L. S., Bucher, J. R., Walker, N. J., and Foster, P. M. (2018). Screening for developmental neurotoxicity at the national toxicology program: The future is here. *Toxicol. Sci.* (forthcoming).

Bjorklund, G., Stejskal, V., Urbina, M. A., Dadar, M., Chirumbolo, S., and Mutter, J. (2018). Metals and Parkinson's disease: Mechanisms and biochemical processes. *Curr. Med. Chem.* **25**, 2198–2214.

Boyd, J. D., Lee-Armandt, J. P., Feiler, M. S., Zaarur, N., Liu, M., Kraemer, B., Concannon, J. B., Ebata, A., Wolozin, B., and Glicksman, M. A. (2014). A high-content screen identifies novel compounds that inhibit stress-induced TDP-43 cellular aggregation and associated cytotoxicity. *J. Biomol. Screen* **19**, 44–56.

Brettschneider, J., Del Tredici, K., Toledo, J. B., Robinson, J. L., Irwin, D. J., Grossman, M., Suh, E., Van Deerlin, V. M., Wood, E. M., Baek, Y., *et al.* (2013). Stages of pTDP-43 pathology in amyotrophic lateral sclerosis. *Ann. Neurol.* **74**, 20–38.

Caragounis, A., Price, K. A., Soon, C. P. W., Filiz, G., Masters, C. L., Li, Q.-X., Crouch, P. J., and White, A. R. (2010). Zinc induces depletion and aggregation of endogenous TDP-43. *Free Radic. Biol. Med.* **48**, 1152–1161.

Carlomagno, Y., Zhang, Y., Davis, M., Lin, W.-L., Cook, C., Dunmore, J., Tay, W., Menkosky, K., Cao, X., Petrucelli, L., *et al.* (2014). Casein kinase II induced polymerization of soluble TDP-43 into filaments is inhibited by heat shock proteins. Kahle PJ, editor. *PLoS One* **9**, e90452.

Chew, J., Gendron, T. F., Prudencio, M., Sasaguri, H., Zhang, Y.-J., Castanedes-Casey, M., Lee, C. W., Jansen-West, K., Kurti, A., Murray, M. E., *et al.* (2015). C9ORF72 repeat expansions in mice cause TDP-43 pathology, neuronal loss, and behavioral deficits. *Science* **348**, 1151–1154.

Crofton, K. M., Mundy, W. R., and Shafer, T. J. (2012). Developmental neurotoxicity testing: A path forward. *Congenit. Anom.* **52**, 140–146.

Das, K., Nag, C., and Ghosh, M. (2012). Familial, environmental, and occupational risk factors in development of amyotrophic lateral sclerosis. *N. Am. J. Med. Sci.* **4**, 350.

Engstrom, A., Wang, H., and Xia, Z. (2015). Lead decreases cell survival, proliferation, and neuronal differentiation of primary cultured adult neural precursor cells through activation of the JNK and p38 MAP kinases. *Toxicol. In Vitro* **29**, 1146–1155.

Fratta, P., Sivakumar, P., Humphrey, J., Lo, K., Ricketts, T., Oliveira, H., Brito-Armas, J. M., Kalmar, B., Ule, A., Yu, Y., *et al.* (2018). Mice with endogenous TDP-43 mutations exhibit gain of splicing function and characteristics of amyotrophic lateral sclerosis. *EMBO. J.* **37**, e98684.

Fritsche, E., Grandjean, P., Crofton, K. M., Aschner, M., Goldberg, A., Heinonen, T., Hessel, E. V. S., Hogberg, H. T., Bennekou, S. H., Lein, P. J., *et al.* (2018). Consensus statement on the need for innovation, transition and implementation of developmental neurotoxicity (DNT) testing for regulatory purposes. *Toxicol. Appl. Pharmacol.* **354**, 3–6.

Fujimura, M., and Usuki, F. (2012). Differing effects of toxicants (methylmercury, inorganic mercury, lead, amyloid, and rotenone) on cultured rat cerebrocortical neurons: Differential expression of Rho proteins associated with neurotoxicity. *Toxicol. Sci.* **126**, 506–514.

Garnier, C., Devred, F., Byrne, D., Puppo, R., Roman, A. Y., Malesinski, S., Golovin, A. V., Lebrun, R., Ninkina, N. N., and Tsvetkov, P. O. (2017). Zinc binding to RNA recognition motif of TDP-43 induces the formation of amyloid-like aggregates. *Sci. Rep.* **7**, 6812.

Garzillo, E. M., Lamberti, M., Genovese, G., Pedata, P., Feola, D., Sannolo, N., Daniele, L., Trojsi, F., Monsurro, M. R., and Miraglia, N. (2014). Blood lead, manganese, and aluminum levels in a regional Italian cohort of ALS patients. *J. Occup. Environ. Med.* **56**, 1062–1066.

Goldstein, L. H., and Abrahams, S. (2013). Changes in cognition and behaviour in amyotrophic lateral sclerosis: Nature of impairment and implications for assessment. *Lancet Neurol.* **12**, 368–380.

de Jong, S. W., Huisman, M. H. B., Sutedja, N. A., van der Kooi, A. J., de Visser, M., Schelhaas, H. J., Fischer, K., Veldink, J. H., and van den Berg, L. H. (2012). Smoking, alcohol consumption, and the risk of amyotrophic lateral sclerosis: A population-based study. *Am. J. Epidemiol.* **176**, 233–239.

Lagier-Tourenne, C., Polymenidou, M., and Cleveland, D. W. (2010). TDP-43 and FUS/TLS: Emerging roles in RNA processing and neurodegeneration. *Hum. Mol. Genet.* **19**, R46–R64.

Li, H.-R., Chiang, W.-C., Chou, P.-C., Wang, W.-J., and Huang, J. (2018). TAR DNA-binding protein 43 (TDP-43) liquid–liquid phase separation is mediated by just a few aromatic residues. *J. Biol. Chem.* **293**, 6090–6098.

Liu-Yesucevitz, L., Lin, A. Y., Ebata, A., Boon, J. Y., Reid, W., Xu, Y.-F., Kobrin, K., Murphy, G. J., Petrucelli, L., and Wolozin, B. (2014). ALS-Linked mutations enlarge TDP-43-enriched neuronal RNA granules in the dendritic arbor. *J. Neurosci.* **34**, 4167–4174.

Malek, A. M., Barchowsky, A., Bowser, R., Heiman-Patterson, T., Lacomis, D., Rana, S., Ada, Y., and Talbott, E. O. (2015). Exposure to hazardous air pollutants and the risk of amyotrophic lateral sclerosis. *Environ. Pollut.* **197**, 181–186.

McGurk, L., Gomes, E., Guo, L., Mojsilovic-Petrovic, J., Tran, V., Kalb, R. G., Shorter, J., and Bonini, N. M. (2018). Poly(ADP-Ribose) prevents pathological phase separation of TDP-43 by promoting liquid demixing and stress granule localization. *Mol. Cell* **71**, 703–717.e9.

Molliex, A., Temirov, J., Lee, J., Coughlin, M., Kanagaraj, A. P., Kim, H. J., Mittag, T., and Taylor, J. P. (2015). Phase separation by low complexity domains promotes stress granule assembly and drives pathological fibrillization. *Cell* **163**, 123–133.

Morozova, N., Weisskopf, M. G., McCullough, M. L., Munger, K. L., Calle, E. E., Thun, M. J., and Ascherio, A. (2008). Diet and amyotrophic lateral sclerosis. *Epidemiology* **19**, 324–337.

Muñoz-Sáez, E., García, E., de, M., Portero, R. M. A., Martínez, A., Alados, M. T. S., and Miguel, B. G. (2015). Analysis of β-N-methylamino-L-alanine (L-BMAA) neurotoxicity in rat cerebellum. *Neurotoxicology* **48**, 192–205.

Murray, M. E., DeJesus-Hernandez, M., Rutherford, N. J., Baker, M., Duara, R., Graff-Radford, N. R., Wszolek, Z. K., Ferman, T. J., Josephs, K. A., Boylan, K. B., *et al.* (2011). Clinical and neuropathologic heterogeneity of c9FTD/ALS associated with hexanucleotide repeat expansion in C9ORF72. *Acta Neuropathol.* **122**, 673–690.

Nakashima-Yasuda, H., Uryu, K., Robinson, J., Xie, S. X., Hurtig, H., Duda, J. E., Arnold, S. E., Siderowf, A., Grossman, M., Leverenz, J. B., *et al.* (2007). Co-morbidity of TDP-43 proteinopathy in Lewy body related diseases. *Acta Neuropathol.* **114**, 221–229.

Neumann, M., Kwong, L. K., Lee, E. B., Kremmer, E., Flatley, A., Xu, Y., Forman, M. S., Troost, D., Kretzschmar, H. A., Trojanowski, J. Q., *et al.* (2009). Phosphorylation of S409/410 of TDP-43 is a consistent feature in all sporadic and familial forms of TDP-43 proteinopathies. *Acta Neuropathol.* **117**, 137–149.

Neumann, M., Sampathu, D. M., Kwong, L. K., Truax, A. C., Micsenyi, M. C., Chou, T. T., Bruce, J., Schuck, T., Grossman, M., Clark, C. M., *et al.* (2006). Ubiquitinated TDP-43 in frontotemporal lobar degeneration and amyotrophic lateral sclerosis. *Science* **314**, 130–133.

Oskarsson, B., Horton, D. K., and Mitsumoto, H. (2015). Potential environmental factors in amyotrophic lateral sclerosis. *Neurol. Clin.* **33**, 877–888.

Patel, A., Lee, H. O., Jawerth, L., Maharana, S., Jahnel, M., Hein, M. Y., Stoynov, S., Mahamid, J., Saha, S., Franzmann, T. M., *et al.* (2015). A liquid-to-solid phase transition of the ALS protein FUS accelerated by disease mutation. *Cell* **162**, 1066–1077.

Polymenidou, M., Lagier-Tourenne, C., Hutt, K. R., Huelga, S. C., Moran, J., Liang, T. Y., Ling, S.-C., Sun, E., Wancewicz, E.,

Mazur, C., *et al.* (2011). Long pre-mRNA depletion and RNA missplicing contribute to neuronal vulnerability from loss of TDP-43. *Nat. Neurosci.* **14**, 459–468.

Prudencio, M., Jansen-West, K. R., Lee, W. C., Gendron, T. F., Zhang, Y.-J., Xu, Y.-F., Gass, J., Stuani, C., Stetler, C., Rademakers, R., *et al.* (2012). Misregulation of human sortilin splicing leads to the generation of a nonfunctional progranulin receptor. *Proc. Natl. Acad. Sci. U.S.A.* **109**, 21510–21515.

Ratti, A., and Buratti, E. (2016). Physiological functions and pathobiology of TDP-43 and FUS/TLS proteins. *J. Neurochem.* **138**, 95–111.

Roos, P. M., Vesterberg, O., Syversen, T., Flaten, T. P., and Nordberg, M. (2013). Metal concentrations in cerebrospinal fluid and blood plasma from patients with amyotrophic lateral sclerosis. *Biol. Trace Elem. Res.* **151**, 159–170.

Ruder, A. M., Hein, M. J., Hopf, N. B., and Waters, M. A. (2014). Mortality among 24,865 workers exposed to polychlorinated biphenyls (PCBs) in three electrical capacitor manufacturing plants: A ten-year update. *Int. J. Hyg. Environ. Health* **217**, 176–187.

Rutherford, N. J., Zhang, Y.-J., Baker, M., Gass, J. M., Finch, N. A., Xu, Y.-F., Stewart, H., Kelley, B. J., Kuntz, K., Crook, R. J. P., *et al.* (2008). Novel mutations in TARDBP (TDP-43) in patients with familial amyotrophic lateral sclerosis. *PLoS Genet.* **4**, e1000193.

Schindelin, J., Arganda-Carreras, I., Frise, E., Kaynig, V., Longair, M., Pietzsch, T., Preibisch, S., Rueden, C., Saalfeld, S., Schmid, B., *et al.* (2012). Fiji: An open-source platform for biological-image analysis. *Nat. Methods* **9**, 676–682.

Shen, A. N., Cummings, C., Hoffman, D., Pope, D., Arnold, M., and Newland, M. C. (2016). Aging, motor function, and sensitivity to calcium channel blockers: An investigation using chronic methylmercury exposure. *Behav. Brain Res.* **315**, 103–114.

Shin, Y., and Brangwynne, C. P. (2017). Liquid phase condensation in cell physiology and disease. *Science* **357**, eaaf4382.

Smirnova, L., Hogberg, H. T., Leist, M., and Hartung, T. (2014). Developmental neurotoxicity – Challenges in the 21st century and in vitro opportunities. *ALTEX* **31**, 129–156.

Squitti, R., Ghidoni, R., Simonelli, I., Ivanova, I. D., Colabufo, N. A., Zuin, M., Benussi, L., Binetti, G., Cassetta, E., Rongioletti, M., *et al.* (2018). Copper dyshomeostasis in Wilson disease and Alzheimer's disease as shown by serum and urine copper indicators. *J. Trace. Elem. Med. Biol.* **45**, 181–188.

Sreedharan, J., Blair, I. P., Tripathi, V. B., Hu, X., Vance, C., Rogelj, B., Ackerley, S., Durnall, J. C., Williams, K. L., Buratti, E., *et al.* (2008). TDP-43 mutations in familial and sporadic amyotrophic lateral sclerosis. *Science* **319**, 1668–1672.

Trojsi, F., Monsurrò, M., and Tedeschi, G. (2013). Exposure to environmental toxicants and pathogenesis of amyotrophic lateral sclerosis: State of the art and research perspectives. *Int. J. Mol. Sci.* **14**, 15286–15311.

Tsao, W., Jeong, Y. H., Lin, S., Ling, J., Price, D. L., Chiang, P.-M., and Wong, P. C. (2012). Rodent models of TDP-43: Recent advances. *Brain. Res.* **1462**, 26–39.

Uryu, K., Nakashima-Yasuda, H., Forman, M. S., Kwong, L. K., Clark, C. M., Grossman, M., Miller, B. L., Kretzschmar, H. A., Lee, V. M.-Y., Trojanowski, J. Q., *et al.* (2008). Concomitant TAR-DNA-binding protein 43 pathology is present in Alzheimer disease and corticobasal degeneration but not in other tauopathies. *J. Neuropathol. Exp. Neurol.* **67**, 555–564.

Vinceti, M., Filippini, T., Mandrioli, J., Violi, F., Bargellini, A., Weuve, J., Fini, N., Grill, P., and Michalke, B. (2017). Lead, cadmium and mercury in cerebrospinal fluid and risk of amyotrophic lateral sclerosis: A case-control study. *J. Trace. Elem. Med. Biol.* **43**, 121–125.

Vinceti, M., Solovyev, N., Mandrioli, J., Crespi, C. M., Bonvicini, F., Arcolin, E., Georgoulopoulou, E., and Michalke, B. (2013). Cerebrospinal fluid of newly diagnosed amyotrophic lateral sclerosis patients exhibits abnormal levels of selenium species including elevated selenite. *Neurotoxicology* **38**, 25–32.

Wang, A., Conicella, A. E., Schmidt, H. B., Martin, E. W., Rhoads, S. N., Reeb, A. N., Nourse, A., Ramirez Montero, D., Ryan, V. H., Rohatgi, R., *et al.* (2018). A single N-terminal phosphomimic disrupts TDP-43 polymerization, phase separation, and RNA splicing. *EMBO. J.* **37**, e97452.

Wang, H., O'Reilly, É. J., Weisskopf, M. G., Logroscino, G., McCullough, M. L., Thun, M. J., Schatzkin, A., Kolonel, L. N., and Ascherio, A. (2011). Smoking and risk of amyotrophic lateral sclerosis: A pooled analysis of 5 prospective cohorts. *Arch. Neurol.* **68**, 207–213.

Wang, M.-D., Gomes, J., Cashman, N. R., Little, J., and Krewski, D. (2014). A meta-analysis of observational studies of the association between chronic occupational exposure to lead and amyotrophic lateral sclerosis. *J. Occup. Environ. Med.* **56**, 1235–1242.

Weisskopf, M. G., Cudkowicz, M. E., and Johnson, N. (2015). Military service and amyotrophic lateral sclerosis in a population-based cohort. *Epidemiology* **26**, 831–838.

Weisskopf, M. G., O'Reilly, E. J., McCullough, M. L., Calle, E. E., Thun, M. J., Cudkowicz, M., and Ascherio, A. (2005). Prospective study of military service and mortality from ALS. *Neurology* **64**, 32–37.